Journal of Materials Chemistry A

Accepted Manuscript

This article can be cited before page numbers have been issued, to do this please use: Y. Kang, N. Yan, Z. Gao, P. Tan, Y. Jiang, X. Liu and L. Sun, *J. Mater. Chem. A*, 2017, DOI: 10.1039/C7TA01069A.

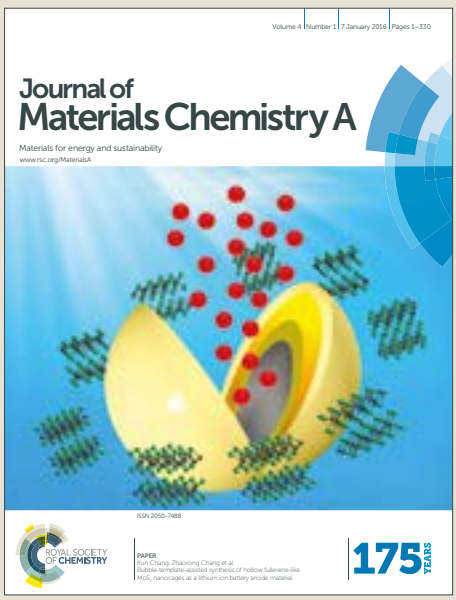

This is an Accepted Manuscript, which has been through the Royal Society of Chemistry peer review process and has been accepted for publication.

Accepted Manuscripts are published online shortly after acceptance, before technical editing, formatting and proof reading. Using this free service, authors can make their results available to the community, in citable form, before we publish the edited article. We will replace this Accepted Manuscript with the edited and formatted Advance Article as soon as it is available.

You can find more information about Accepted Manuscripts in the author guidelines.

Please note that technical editing may introduce minor changes to the text and/or graphics, which may alter content. The journal's standard Terms & Conditions and the ethical guidelines, outlined in our author and reviewer resource centre, still apply. In no event shall the Royal Society of Chemistry be held responsible for any errors or omissions in this Accepted Manuscript or any consequences arising from the use of any information it contains.

ROYAL SOCIETY OF CHEMISTRY

rsc.li/materials-a

View Article Online
DOI: 10.1039/C7TA01069A

Journal Name

COMMUNICATION

Controllable Construction of Metal-Organic Polyhedra in Confined Cavities via In Situ Sites-Induced Assembly

Received 00th January 20xx,
Accepted 00th January 20xx

DOI: 10.1039/x0xx00000x

www.rsc.org/

Ying-Hu Kang, Ni Yan, Zhen-Yu Gao, Peng Tan, Yao Jiang, Xiao-Qin Liu, and Lin-Bing Sun*

Poor dispersity and low stability are two predominant shortcomings hindering the applications of metal-organic polyhedra (MOPs). The confinement of MOPs in nanoscale cavities of mesoporous matrices is efficient in overcoming both shortcomings, while the improvement of the current double-solvent method is highly expected. Here we develop a facile, controllable strategy to fabricate three MOPs (coordinated from dicopper and carboxylates) in confined cavities via in situ sites-induced assembly (SIA), for the first time. The cavities of mesoporous matrix SBA-16 were pre-functionalized with amine sites, which induce in situ assembly of precursors that diffused into cavities. Hence, both amount and location of MOPs in the mesoporous matrix can be easily controlled. Upon confinement, the dispersity, stability, and catalytic performance (on ring-opening reactions) of MOPs are greatly improved. Moreover, the enhancement of stability makes it possible to observe MOPs using high-resolution transmission electron microscopy (HRTEM) directly.

Metal-organic polyhedra (MOPs, also called molecular nanocages and nanoballs) are a class of inorganic-organic discrete coordination complexes constructed from metal ions and highly directional ligands.[1-10] Because of their intriguing structure, MOPs show high potentials in applications varied from adsorption and catalysis to biological self-assembly.[11-24] Nevertheless, these applications are seriously obstructed by two shortcomings, that is, poor dispersity and low stability of MOPs.[25-28] On the one hand, MOPs are prone to aggregate in solid state during activation for the removal of solvent molecules, although some MOPs can be well dispersed in solution. Such an activation process is necessary for both metal-organic frameworks (MOFs) and MOPs prior to use.[29-34] Because MOFs possess interconnected channels, activation improves the accessibility of their active sites greatly.[35-37] However, MOP molecules tend to aggregate in solid state after activation, which results in the blockage of active sites and compromises the catalytic and adsorptive activity of MOPs severely. On the other hand, the stability of MOPs is weak since they are fabricated by coordination bonds.[38-40] The structure of some MOPs can be degraded even in the presence of trace levels of water.

To overcome the shortcomings, the confinement of MOPs in porous matrices including MOFs and mesoporous silica was reported recently by Li's group[41] and ours.[38] In our case, MOP

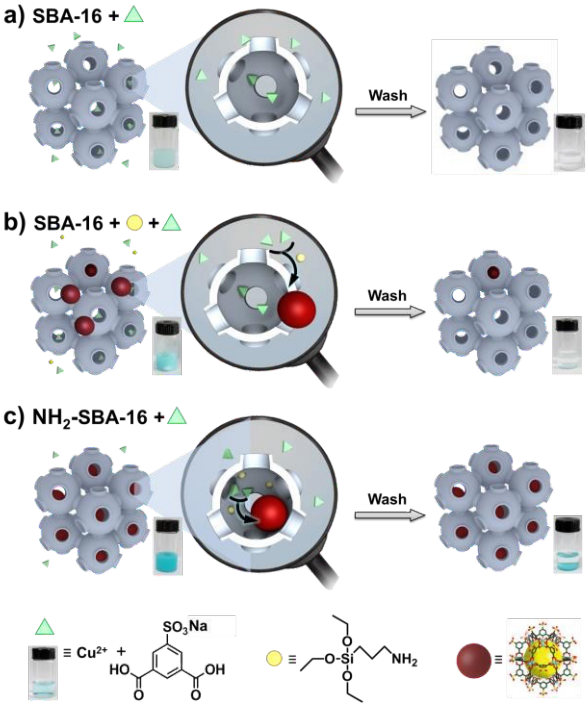

Scheme 1. Comparison of three different synthetic processes through adding (a) SBA-16, (b) SBA-16 and the inducer APTES, and (c) NS to the precursor solution of MOP**1**.

State Key Laboratory of Materials-Oriented Chemical Engineering, Jiangsu National Synergetic Innovation Center for Advanced Materials, College of Chemistry and Chemical Engineering, Nanjing Tech University, Nanjing 210009, China. E-mail: lbsun@njtech.edu.cn.

†Electronic Supplementary Information (ESI) available: Full details of sample preparation, characterizations and additional data. See DOI: 10.1039/x0xx00000x

View Article Online
DOI: 10.1039/C7TA01069A

molecules were introduced to a three-dimensional cavity-structured mesoporous matrix (SBA-16). This mesoporous matrix has large cavities (~6 nm) interconnected by small pore entrances (~2 nm).[42-43] Our MOPs with a dimension of ~3 nm are just between the size of cavities and pore entrances. As a result, MOPs are confined in the cavities, which produces isolated molecules with obviously enhanced dispersity and stability and overcomes both shortcoming of MOPs. In the previous study, however, a double-solvent method was employed, in which porous matrices were dispersed in a hydrophobic solvent, followed by addition of a tiny amount of hydrophilic precursor solution and a basic inducer.[38] The volume of precursor solution must be smaller than the pore volume of porous matrix, so that the hydrophilic precursor solution is able to enter the pores through capillary force.[38, 41, 44] It should be stated that there are several defects for the confinement of MOPs by the double-solvent method. First, the synthetic system is sort of complicated due to the use of two incompatible solvents. Second, all precursors must be dissolved in a small quantity of solvents ($V_{solution} < V_{pore}$), and thus the amount of introduced MOPs is dependent on the solubility of precursors. Third, the diffusion of both precursor and inducer molecules in pores matters for the assembly caused by inducer, which makes the synthetic process hard to control. Taking into account that the confinement is highly efficient in improving MOP properties, the development of a facile, controllable method to introduce MOPs to confined spaces is extremely desirable.

Here we report for the first time a facile, controllable strategy to fabricate MOPs in confined cavities via in situ sites-induced assembly (SIA, Scheme 1). The cavities of mesoporous matrix SBA-16 were pre-functionalized with amine sites, which act as the inducer and trigger in situ assembly of precursors in the cavities. The present SIA strategy has several advantages over the double-solvent one. First, the synthetic system is simplified since only one solvent is involved, and there is no strict requirements on the properties of solvents. Second, the solubility of precursors is not a problem any longer, and large amounts of solvents can be used while the formation of MOPs only occurs for the precursor molecules diffused into the cavities in which there are inducer sites. Third, the inducer sites are already immobilized on the cavities, and only diffusion of precursor molecules matters, making the synthesis easy to control. As a result, both amount and location of MOPs in the mesoporous matrix can be well controlled by means of the SIA strategy. Because the dimension of MOPs (~3 nm) is smaller than the size of cavities (~6 nm) but larger than the size of pore entrances (~2 nm), the formed MOPs are isolated in the cavities. The high dispersity makes the active sites of MOPs pretty accessible, and the catalytic activity of isolated MOPs is much higher than that of aggregated bulk MOPs. Moreover, the confinement enhances the stability of MOPs. Upon exposure to humid environment, MOPs in confined cavities maintain the structure and catalytic activity well, whereas the structure and catalytic activity of bulk MOPs are degraded evidently. It is worth noting that the enhancement of stability makes it possible to observe MOPs directly using high-resolution transmission electron microscopy (HRTEM), although MOPs are very sensitive to the high-energy electron beam.

As a proof of concept, we first employed MOP**1** constructed from $Cu(NO_3)_2$ and 5-sulfoisophthalic acid sodium salt (H_2L1, Scheme S1).[45] MOP**1** shows a cuboctahedral geometry when the twelve dicopper units are regarded as vertices and the linkers as edges. Amine-functionalized mesoporous silica NH_2-SBA-16 (NS) was prepared by a co-condensation approach using (3-aminopropyl)triethoxysilane (APTES). In a typical SIA process, the mesoporous matrix NS was added to the precursor solution containing $Cu(NO_3)_2$ and H_2L1 (Scheme 1). After 0.5 h of stirring, the blue solids were separated by centrifugation and wash twice with methanol. The obtained composites resulted from an increasing dosage of precursors were denoted as M**1**N-1, M**1**N-2, M**1**N-3, and M**1**N-4, corresponding to 0.7, 1.6, 2.9, and 3.1 MOPs per cavity, respectively, from inductively coupled plasma (ICP) results. Although the dosage of precursors for M**1**N-4 is 1.5 times higher than that for M**1**N-3, the content of MOPs is similar in the final composites. This implies that the maximum loading in the present case is about 3 MOPs per cavity.

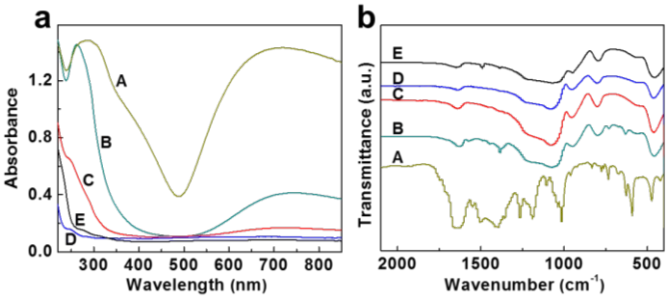

Fig. 1 (a) UV-vis and (b) IR spectra. (A) MOP**1**; (B) the sample synthesized by adding NS to the precursor solution of MOP**1**; (C) the sample synthesized by adding SBA-16 and APTES to the precursor solution of MOP**1**; (D) the sample synthesized by adding SBA-16 to the precursor solution of MOP**1**; (E) NS.

Two control experiments were run to examine the validity of SIA strategy. Owing to the absence of inducer, no MOP is formed if unfunctionalized SBA-16 is added to the precursor solution (Scheme 1a). Further addition of the inducer APTES to the above system, MOPs can be produced (Scheme 1b). However, most MOPs locate outside the pores and can be removed after washing with methanol (MOP**1** is soluble in methanol). The very slight blue color of the resultant sample indicates a tiny amount of MOPs are introduced to the cavities. Interestingly, MOPs are selectively fabricated in the cavities in the presence of NS, and the final sample is blue even after thorough washing (Scheme 1c). These results reveal that the precursors can diffuse into the cavities of NS, and the amine sites in the cavities are efficient in inducing in situ formation of MOPs. Also, pre-functionalization with inducer sites favors the selective formation of MOPs in the cavities, while most MOPs are formed outside the cavities if the foreign inducer is utilized. Various techniques were used to characterize the formed MOPs. In the UV-vis spectra, no absorption peaks are observed for mesoporous matrix NS, due to the absence of absorption for

View Article Online
DOI: 10.1039/C7TA01091A

tetrahedral coordinated SiO_4 framework (Fig. 1a). MOP**1** has a strong absorption peak at 730 nm, which is caused by dicopper paddle-wheel structure.[45] For the sample prepared by adding SBA-16 to the precursor solution, no absorption for MOPs appears. Further addition of the inducer leads to the generation of a weak absorption peak at 730 nm, indicating the formation of a small amount of MOPs. Noteworthily, an obvious absorption of MOPs becomes visible in the presence of NS, which gives further evidence of MOPs formation. Similar trend is also observed from infrared (IR) spectra (Fig. 1b). Due to the overlapped IR bands of MOPs and the support silica, some characteristic bands of MOPs are not obvious. However, the bands of MOP**1** can be identified in the composite derived from NS. Moreover, the intensity of both UV-vis and IR peaks increases gradually with the rise of MOP content in the composites (Figs. S1 and S2). The composites M**1**N-3 and M**1**N-4 show comparable peak intensity, which confirms the similar content of MOPs.

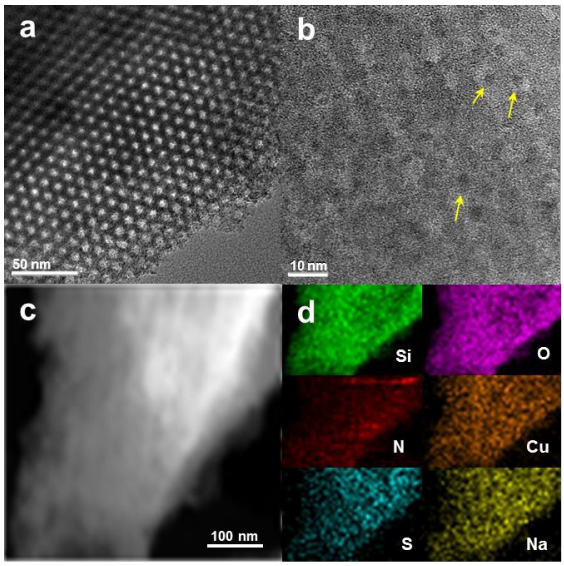

Fig. 2 (a) TEM, (b) HRTEM, (c) STEM, and (d) elemental mapping of the composite M**1**N-3. The arrows in b show several examples of MOPs.

TEM characterization provides information on both mesoporous matrix and MOPs. TEM images of all composites exhibit ordered mesoporous structure (Figs. 2 and S3-S5), which is analogous to the original mesoporous matrix NS (Fig. S6). Also, the pore regularity of the composites containing MOPs is well supported by the low-angle powder X-ray diffraction (PXRD) patterns (Fig. S7). These results demonstrate that the periodic ordering of mesostructure is well retained after introducing MOPs. HRTEM technique was also attempted to investigate the composites. Because MOPs are normally fairly sensitive to the high-energy electron beam, the report concerning direct observation of MOPs through TEM is very scarce. Surprisingly, some spherical nanoparticles, which are believed to originate from MOPs considering the size and location, can be well distinguished from the HRTEM image (Fig. 2b). It is apparent that the confinement of MOPs in the cavities of mesoporous matrix enhances their stability, making it possible to observe MOPs directly by means of TEM. Elemental mapping was also employed to examine the distribution of MOPs in mesoporous matrix. For the mesoporous matrix NS, Si and O stemmed from the silica framework as well as N from amine groups are detected (Fig. S6). Besides Si, O, and N from the matrix NS, the elements Cu, S, and Na come from MOP**1** are observed (Figs. 2 and S3-S5). Furthermore, the elements are distributed in the whole composite homogeneously in spite of different MOP contents. In scanning electron microscopy (SEM) images, the matrix NS shows lump-like morphology, while MOP presents flake-like morphology (Fig. S8). In the case of composites, the morphology of NS is well preserved and no flake-like material is observed. This suggests that MOPs are mainly located inside the pores of mesoporous matrix. The wide-angle PXRD pattern of pristine NS exhibits a broad peak at around 23°, which is attributed to amorphous silica framework (Fig. S9). It is worthy of note that all MOPs-containing composites give the identical patterns to pristine NS, which is apparently different from aggregated bulk MOPs with obvious diffraction peaks. On the basis of these results, it is obvious that MOPs are well dispersed in the mesoporous matrix.

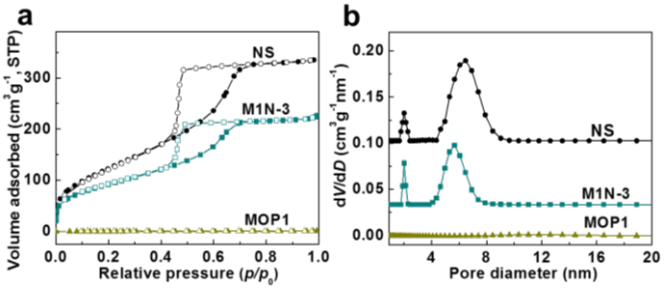

Fig. 3 (a) N_2 sorption isotherms and (b) PSDs of MOP**1**, NS, and their composite M1N-3.

The change of pore structure was studied by N_2 adsorption at 77 K. Because bulk MOPs tend to aggregate, the uptake of N_2 is negligible (Fig. 3). The MOP-containing composites give a type-IV isotherm and an H2-type hysteresis loop, which is analogous to the mesoporous matrix NS (Figs. 3 and S10). In contrast to pristine NS, the hysteresis loop moves to relatively low pressures after introducing MOPs. The results of pore size distributions (PSDs) provide further evidence of MOP location. The matrix NS presents two types of pores centered at 2.0 and 6.4 nm, which originates from pore entrances and cavities respectively. Interestingly, the incorporation of MOPs results in the decline of cavity size from 6.4 to 5.6 nm (for M**1**N-3), whereas the entrance size keeps constant (Table S1). In addition to M1N-3, the composites with different MOP contents also show a similar tendency. These results apparently demonstrate that MOPs are selectively constructed in the cavities of mesoporous matrix rather than the entrances, which plays an important role in the generation of isolated MOPs in the confined space.

The obtained composites were used to catalyze the ring-opening of styrene oxide (SO) to synthesize 2-methoxy-2-phenylethanol (MPE), which is a useful intermediate for both

View Article Online
DOI: 10.1039/C7TA01069A

chemical and pharmaceutical industries.[46-47] Traditionally, the ring-opening of styrene oxide is catalyzed by homogeneous acids or bases, leading to the problem of waste production and the difficulty in separation. The substitution of conventional homogeneous catalysts with heterogeneous ones thus attracts increasing attention. MOPs possess coordinatively unsaturated metal sites, which may be active for ring-opening reactions. Negligible amount of SO is converted over pristine NS (Fig. 4a). Under the catalysis of MOP**1**, the yield of MPE is 39% at 120 min, suggesting the presence of active sites. It is interesting to note that the yield of MPE reaches 80% over the composite M**1**N-3, which is apparently higher than that catalyzed by individual mesoporous matrix and MOPs. Recyclability is of great importance for the practical applications, and the present heterogeneous catalysts are thus recovered after reactions and reused (Fig. 4b). No loss in activity is observed for the composite in the four successive cycles. Nonetheless, the yield of MPE over MOP**1** decreases harshly (from 40 % to 3 %) in the second cycle. These results clearly show that isolated MOPs are much more active and stable than aggregated bulk ones.

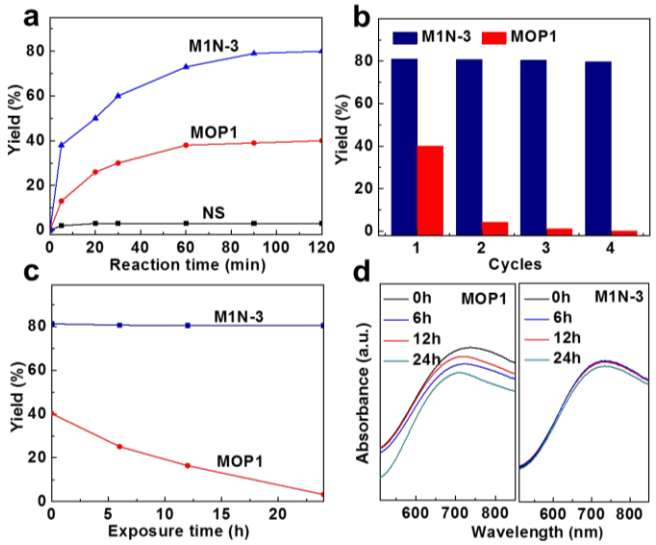

Fig. 4 (a) The ring-opening of styrene oxide catalyzed by MOP**1**, NS, and their composite M**1**N-3. (b) Reusability of MOP**1** and M**1**N-3. (c) Catalytic capacity and (d) UV-vis spectra of MOP**1** and M**1**N-3 upon exposure to humid atmosphere.

To further evaluate the stability, the materials were exposed to humid environment (relative humidity = 50%). The materials after exposure were used for catalysis and subjected to structure characterization. Upon exposure to humid environment (Fig. 4c), the yield of MPE is reduced sharply from 40% to 16% (12 h) and 3% (24 h). However, under the identical treatment conditions, the composite exhibits a constant activity in catalysis. UV-vis spectra show that for the MOPs after exposure, the absorption peak derived from dicopper paddle-wheel units shifts from 730 to 700 nm, which means the degradation of MOP structure (Fig. 4d). In the case of the composite, nevertheless, the absorption at 730 nm keeps unchanged after exposure for even 24 h. This is in good agreement with the catalytic results, pointing out the stability of MOPs is evidently enhanced upon confinement in nanoscale cavities.

Besides MOP**1**, two other MOPs (i.e. MOP**2** and MOP**3**, Scheme S1) with the same geometry but different ligand functionality (i.e. hydroxyl and *tert*-butyl) were also confined in the mesoporous matrix NS by use of SIA. The formation of MOPs in NS can be observed visibly from the color change (Figs. S11 and S12). TEM images imply that the ordered mesostructure of NS is well preserved after the introduction of MOPs (Figs. S13 and S14). UV-vis spectra give further evidence of the successful formation of MOPs (Figs. S15 and S16), which are homogeneously distributed in the matrix (see elemental mappings). The high dispersion of MOPs in NS is also confirmed by wide-angle PXRD patterns, in which no diffraction peaks ascribed to MOPs appear (Figs. S17 and S18). The PSD results show that the cavity size declines while the entrance size keeps constant (Figs. S19 and S20), which demonstrates the selective fabrication of MOPs in cavities of NS. These results prove that the SIA strategy is efficient in introducing different MOPs to mesoporous matrix.

Conclusions

In summary, we demonstrate the successful fabrication of MOPs in the confined nanoscale cavities by using the SIA strategy. The pre-functionalized amine sites function as the inducer, trigger in situ assembly of precursors in the cavities, and avoid the formation of MOPs outside the pores. Isolated MOPs with unusual dispersity are thus formed, which makes the active sites of MOPs pretty accessible, and the catalytic activity of isolated MOPs is much higher than that of aggregated bulk MOPs. Moreover, upon confinement, the stability of MOPs is greatly enhanced. After exposure to humid environment, MOPs in confined cavities maintain the structure and catalytic activity well, whereas the structure and catalytic activity of bulk MOPs are degraded seriously. Also, the enhanced stability makes it possible to observe MOPs using TEM technique directly. The present SIA strategy may open up an avenue for the confinement of various MOPs as well as other supramolecular architectures in nanoscale spaces, leading to the fabrication of isolated architectures with enhanced stability and dispersity that are highly expected for various applications but impossible to achieve for their bulk analogues.

Acknowledgements

This work was supported by the National Natural Science Foundation of China (21576137), the Distinguished Youth Foundation of Jiangsu Province (BK20130045), the Fok Ying-Tong Education Foundation (141069), and the Project of Priority Academic Program Development of Jiangsu Higher Education Institutions.

Notes and references

1 T. R. Cook and P. J. Stang, *Chem. Rev.*, 2015, **115**, 7001.

2 R. Chakrabarty, P. S. Mukherjee and P. J. Stang, *Chem. Rev.*, 2011, **111**, 6810.
3 W. J. Ramsay, F. T. Szczypiński, H. Weissman, T. K. Ronson, M. M. J. Smulders, B. Rybtchinski and J. R. Nitschke, *Angew. Chem. Int. Ed.*, 2015, **54**, 5636.
4 S.-T. Zheng, T. Wu, B. Irfanoglu, F. Zuo, P. Feng and X. Bu, *Angew. Chem. Int. Ed.*, 2011, **50**, 8034.
5 J. M. Teo, C. J. Coghlan, J. D. Evans, E. Tsivion, M. Head-Gordon, C. J. Sumby and C. J. Doonan, *Chem. Commun.*, 2016, **52**, 276.
6 D. Kim, X. F. Liu and M. S. Lah, *Inorg. Chem. Front.*, 2015, **2**, 336.
7 T.-H. Chen, L. Wang, J. V. Trueblood, V. H. Grassian and S. M. Cohen, *J. Am. Chem. Soc.*, 2016, **138**, 9646.
8 H. Furukawa, J. Kim, N. W. Ockwig, M. O'Keeffe and O. M. Yaghi, *J. Am. Chem. Soc.*, 2008, **130**, 11650.
9 H. Furukawa, J. Kim, K. E. Plass and O. M. Yaghi, *J. Am. Chem. Soc.*, 2006, **128**, 8398.
10 S. Leininger, B. Olenyuk and P. J. Stang, *Chem. Rev.*, 2000, **100**, 853.
11 Y. Kohyama, T. Murase and M. Fujita, *J. Am. Chem. Soc.*, 2014, **136**, 2966.
12 M. Fujita, *Chem. Soc. Rev.*, 1998, **27**, 417.
13 M. Yoshizawa, J. K. Klosterman and M. Fujita, *Angew. Chem. Int. Ed.*, 2009, **48**, 3418.
14 K. Takao, K. Suzuki, T. Ichijo, S. Sato, H. Asakura, K. Teramura, K. Kato, T. Ohba, T. Morita and M. Fujita, *Angew. Chem. Int. Ed.*, 2012, **51**, 5893.
15 D. Zhao, S. W. Tan, D. Q. Yuan, W. G. Lu, Y. H. Rezenom, H. L. Jiang, L. Q. Wang and H. C. Zhou, *Adv. Mater.*, 2011, **23**, 90.
16 B. Li, Y. Zhang, D. Ma, T. Ma, Z. Shi and S. Ma, *J. Am. Chem. Soc.*, 2014, **136**, 1202.
17 J. Park, L. B. Sun, Y. P. Chen, Z. Perry and H. C. Zhou, *Angew. Chem. Int. Ed.*, 2014, **53**, 5842.
18 Q. G. Zhai, C. Y. Mao, X. Zhao, Q. P. Lin, F. Bu, X. T. Chen, X. H. Bu and P. Y. Feng, *Angew. Chem. Int. Ed.*, 2015, **54**, 7886.
19 Y. T. Li, D. J. Zhang, F. Y. Gai, X. Q. Zhu, Y. N. Guo, T. L. Ma, Y. L. Liu and Q. S. Huo, *Chem. Commun.*, 2012, **48**, 7946.
20 N. Ahmad, H. A. Younus, A. H. Chughtai and F. Verpoort, *Chem. Soc. Rev.*, 2015, **44**, 9.
21 N. Ahmad, A. H. Chughtai, H. A. Younus and F. Verpoort, *Coord. Chem. Rev.*, 2014, **280**, 1.
22 A. Schmidt, A. Casini and F. E. Kuhn, *Coord. Chem. Rev.*, 2014, **275**, 19.
23 H. Vardhan, M. Yusubov and F. Verpoort, *Coord. Chem. Rev.*, 2016, **306**, 171.
24 J. Roukala, J. Zhu, C. Giri, K. Rissanen, P. Lantto and V.-V. Telkki, *J. Am. Chem. Soc.*, 2015, **137**, 2464.
25 N. Hosono, M. Gochomori, R. Matsuda, H. Sato and S. Kitagawa, *J. Am. Chem. Soc.*, 2016, **138**, 6525.
26 T. F. Liu, Y. P. Chen, A. A. Yakovenko and H. C. Zhou, *J. Am. Chem. Soc.*, 2012, **134**, 17358.
27 Z. Lu, C. B. Knobler, H. Furukawa, B. Wang, G. N. Liu and O. M. Yaghi, *J. Am. Chem. Soc.*, 2009, **131**, 12532.
28 L. B. Sun, J. R. Li, W. G. Lu, Z. Y. Gu, Z. P. Luo and H. C. Zhou, *J. Am. Chem. Soc.*, 2012, **134**, 15923.
29 A. Mallick, B. Garai, D. D. Diaz and R. Banerjee, *Angew. Chem. Int. Ed.*, 2013, **52**, 13755.
30 U. Stoeck, I. Senkovska, V. Bon, S. Krause and S. Kaskel, *Chem. Commun.*, 2015, **51**, 1046.
31 Z. Niu, S. Fang, X. Liu, J. G. Ma, S. Q. Ma and P. Cheng, *J. Am. Chem. Soc.*, 2015, **137**, 14873.
32 J. An, O. K. Farha, J. T. Hupp, E. Pohl, J. I. Yeh and N. L. Rosi, *Nat. Commun.*, 2012, **3**, 604.
33 S. Pasquale, S. Sattin, E. C. Escudero-Adan, M. Martinez-Belmonte and J. de Mendoza, *Nat. Commun.*, 2012, **3**, 785.
34 J. R. Li, J. M. Yu, W. G. Lu, L. B. Sun, J. Sculley, P. B. Balbuena and H. C. Zhou, *Nat. Commun.*, 2013, **4**, 893.
35 Y. Han, J. R. Li, Y. B. Xie and G. S. Guo, *Chem. Soc. Rev.*, 2014, **43**, 5952.
36 J. J. Perry, J. A. Perman and M. J. Zaworotko, *Chem. Soc. Rev.*, 2009, **38**, 1400.
37 L. E. Darago, M. L. Aubrey, C. J. Yu, M. I. Gonzalez and J. R. Long, *J. Am. Chem. Soc.*, 2015, **137**, 15703.
38 Y.-H. Kang, X.-D. Liu, N. Yan, Y. Jiang, X.-Q. Liu, L.-B. Sun and J.-R. Li, *J. Am. Chem. Soc.*, 2016, **138**, 6099.
39 L. Lu, X.-Y. Li, X.-Q. Liu, Z.-M. Wang and L.-B. Sun, *J. Mater. Chem. A*, 2015, **3**, 6998.
40 D.-D. Zu, L. Lu, X.-Q. Liu, D.-Y. Zhang and L.-B. Sun, *J. Phys. Chem. C*, 2014, **118**, 19910.
41 X. Qiu, W. Zhong, C. H. Bai and Y. W. Li, *J. Am. Chem. Soc.*, 2016, **138**, 1138.
42 H. Q. Yang, L. Zhang, L. Zhong, Q. H. Yang and C. Li, *Angew. Chem. Int. Ed.*, 2007, **46**, 6861.
43 D. Y. Zhao, Q. S. Huo, J. L. Feng, B. F. Chmelka and G. D. Stucky, *J. Am. Chem. Soc.*, 1998, **120**, 6024.
44 A. Aijaz, A. Karkamkar, Y. J. Choi, N. Tsumori, E. Ronnebro, T. Autrey, H. Shioyama and Q. Xu, *J. Am. Chem. Soc.*, 2012, **134**, 13926.
45 J. R. Li and H. C. Zhou, *Nat. Chem.*, 2010, **2**, 893.
46 G. D. Yadav and S. Singh, *Tetrahedron Lett.*, 2014, **55**, 3979.
47 M. Tokunaga, J. F. Larrow, F. Kakiuchi and E. N. Jacobsen, *Science*, 1997, 277, 936.

View Article Online
DOI: 10.1039/C7TA01069A

Table of Contents

Controllable Construction of Metal-Organic Polyhedra in Confined Cavities via In Situ Sites-Induced Assembly

Ying-Hu Kang, Ni Yan, Zhen-Yu Gao, Peng Tan, Yao Jiang, Xiao-Qin Liu, and Lin-Bing Sun*

State Key Laboratory of Materials-Oriented Chemical Engineering, Jiangsu National Synergetic Innovation Center for Advanced Materials, College of Chemistry and Chemical Engineering, Nanjing Tech University, Nanjing 210009, China.

Controllable fabrication of metal-organic polyhedra in confined cavities with improved properties was realized through in situ sites-induced assembly.